Kinetic study of rare earth elements extraction from decrepitated magnet powder using liquid magnesium

Nicolas Stankovic, Julien Jourdan, Jérôme Marin, Alexandre Chagnes, Thibault Quatravaux

ARTICLE

Kinetic study of rare earth elements extraction from decrepitated magnet powder using liquid magnesium

Received 00th January 20xx,
Accepted 00th January 20xx

DOI: 10.1039/x0xx00000x

Nicolas Stankovic[a,b], Julien Jourdan[b], Jérôme Marin[a], Alexandre Chagnes[a], Thibault Quatravaux[b*]

This study presents a comprehensive investigation of neodymium extraction from decrepitated magnet powder using liquid magnesium. Neodynium extraction from the decrepitated magnet into the liquid magnesium was assessed between 700 and 900 °C by measuring the average length of the diffusion zone in sintered samples of 3 mm-thickness. Experiments were performed in a reactor which the design ensured a homogeneous distribution of magnesium through efficient agitation. An empirical model was used to model the growth kinetics of the diffusion zone by using the Rosin-Rammler equation to estimate particle size distribution. The results were extrapolated to decrepitated magnet powder particles to simulate the neodymium extraction performances. Remarkably, the treatment time required was relatively short, not exceeding 22 minutes, and varied depending on the extraction target and temperature. Both the temperature and the setpoint for the volume rate to be treated emerged as critical factors. Their impact on the process was thoroughly examined and discussed. These findings offer promising insights into the industrial feasibility of the use of liquid magnesium for rare-earth extraction from spent permanent magnet.

1. Introduction

Since their invention in 1983, neodymium-iron-boron (NdFeB) magnets have become key technological components due to their significantly higher stored volumetric magnetic energy compared to ferrite-based (15 times more), samarium-cobalt (2.5 times more) and AlNiCo (7 times more) permanent magnets[1]. These remarkable properties make them indispensable for producing small and powerful magnets for critical applications such as electronics (hard drives), transportation (hybrid and electric vehicles), and energy (wind turbines), which cover more than half of the world's permanent magnet market[2].

NdFeB magnets mainly contain 60-70 % (wt) iron, 20-25 % (wt) neodymium coupled with 0-5% (wt) praseodymium, 1 % (wt) boron and 0-5 % (wt) dysprosium which extends operating temperature range of the magnets up to 200 °C, as well as traces of other elements to improve the magnet performances such as cobalt, nickel and copper. A report written by the Joint Research Centre and the European commission's science and knowledge service[3] indicated that the global cumulative demand for neodymium, praseodymium, terbium and dysprosium was approximately 50 kt in 2018 including 40 kt of neodymium. Another report published by The International Renewable Energy Agency[4] mentioned that the amount needed for magnet production could grow from 50 kt to 225 kt per year including 180 kt for electric vehicles and 50 kt for wind turbines. In order to mitigate the supply risk (deficit of 135 kt of NdFeB magnets by the end of this decade), many projects focus on the exploitation of new deposits in Nordic countries, Turkey, Canada and Australia. Furthermore, although magnet recycling will not contribute sufficiently in magnet production, recycling remains a good opportunity to reduce the supply risk of REEs.

However, a special attention must be paid to the development of the recycling industry, particularly in Europe where there is almost no mining activity, in Japan and in the United States. Therefore, many governments have recently invested in the rare-earth recycling industry so that NdFeB magnets could contribute as secondary resources for neodymium and dysprosium since recycling could provide up to 2500 tons annum[5].

To meet this need and match with the development of the circular economy, promising recycling routes are already under development (figure 1). The short-loop recycling route (Figure 1, route a) appears as one of the most interesting routes. New NdFeB magnets can be produced from spent magnets by hydrogen decrepitation (HD) or other technologies and sintering of the resulting powder[6]. The HD process (embrittlement of the alloy by hydrogen absorption) is applied to end-of-life sintered magnets in order to produce a powder suitable for further reprocessing to make new magnet by sintering at high temperature and compaction under magnetic field. The main goal in this case is to avoid any degradation of the powder (oxidation is highly detrimental to the magnet properties) and to maintain, as much as possible, the existing microstructure in the powder, in order to recover magnetic

[a] University of Lorraine, CNRS, GeoRessources, F-54000 Nancy, France.
[b] University of Lorraine, CNRS, Institut Jean Lamour, F-54000 Nancy, France.
*Corresponding author: Thibault Quatravaux (thibault.quatravaux@univ-lorraine.fr)

Footnotes relating to the title and/or authors should appear here.
Electronic Supplementary Information (ESI) available: [details of any supplementary information available should be included here]. See DOI: 10.1039/x0xx00000x

performances close to those of pristine magnets. Besides, the HD process can also be applied as a pre-treatment step for further long-loop recycling processes in order to increase their kinetics for extraction of rare-earth elements trough pyrometallurgical and/or hydrometallurgical processes[7–11]. Hydrogenation Disproportionation Desorption Recombination (HDDR) process is also an extension of the HD process. The HDDR process offers a promising multistage approach to produce anisotropic powders. The initial stage comprises the exothermic hydrogenation of both the rare-earth elements (REE)-rich grain boundary phase and the $Nd_2Fe_{14}B$ phase through interstitial absorption of hydrogen. The subsequent stage involves the exothermic disproportionation of the $Nd_2Fe_{14}BH_x$ phase above 600 °C. Following the disproportionation stage, a high-temperature desorption stage occurs, where hydrogen is removed as the reactor is emptied. The final stage encompasses the recombination of the $Nd_2Fe_{14}B$ phase, which is a high-temperature endothermic process[12–18].

The following reversible reactions describe the HDDR process:

$$Nd_2Fe_{14}B + 2H_2 \rightarrow 2NdH_2 + 12Fe + Fe_2B$$
HD process

$$2NdH_2 + 12Fe + Fe_2B \rightarrow Nd_2Fe_{14}B + 2H_2$$
DR process

More traditionally, the hydrometallurgical route (Figure 1, route b) allows the recovery of rare-earth elements by combining leaching, solvent extraction, ion exchange and/or precipitation. These techniques implemented for the recovery of REEs from NdFeB magnets are similar to those used in the hydrometallurgical treatment of ores[19] and are subject of extensive research to increase metal extraction efficiency and mitigate environmental impacts. A thermal oxidative pre-treatment offers selectivity during the leaching step by avoiding iron dissolution. The decrease of iron concentration in leaching solution is particularly important as the recovery of REEs in the presence of iron is a great challenge in the purification step (liquid-liquid extraction, solid-liquid extraction, precipitation). After liquid-liquid extraction or solid-liquid extraction, precipitation of REEs can be performed to produce sulfate or oxalate salts. These salts have to be converted into metals to make new magnets. As mentioned above, magnets do not contain only neodymium, iron and boron, but also other elements such as praseodymium, dysprosium, nickel, cobalt, copper, etc. In some cases, the co-valorization of these metals could be of great interest while iron could be reused in steelmaking industry.

The Liquid Metal Extraction (LME) process (Figure 1, route c) has been recently investigated to extract REEs from magnets[20]. LME is based on solid-liquid extraction using a molten metal, mainly magnesium that acts as high-temperature solvent due to its strong chemical affinity towards REEs. The liquid magnesium extraction process could rely on the two following steps: (i) diffusion of rare-earth elements contained in the magnets by immersion in liquid magnesium and (ii) distillation of magnesium and recovery of metallic rare-earth elements. In a short-loop process, magnesium can be reused in LME after distillation, and iron-based alloy can be reintroduced in the steelmaking industry. Such an operation in a magnet recycling process may reduce effluent generation and environmental impacts. Therefore, LME process may be far less harmful toward the environment than mining as it can be considered as an effluent-free process. Its process cost depends mainly on magnesium consumption and the energy used to maintain magnesium at a liquid state. The main advantage of this process beside the absence of effluent is the direct production of rare-earth metals, which can be used directly to produce new magnets.

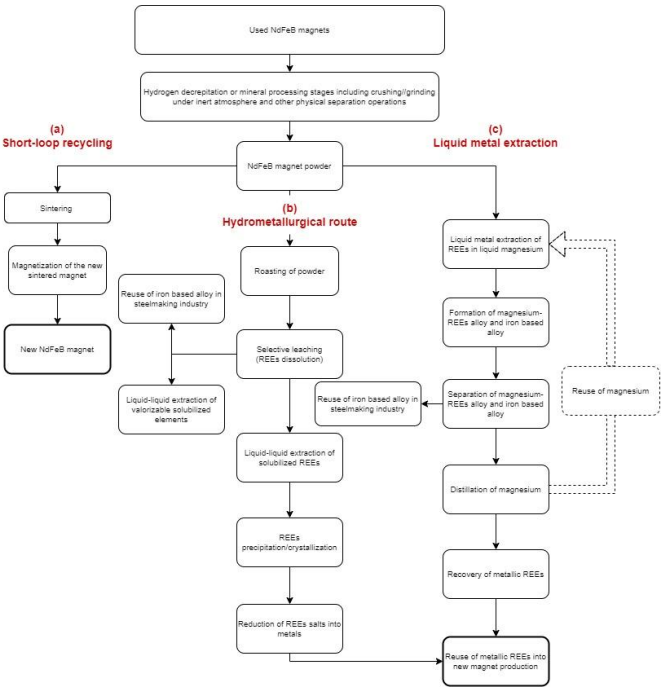

Figure 1: Recycling routes of REEs from NdFeB magnets

Xu et al.[21] and Chae et al.[22] studied the diffusion of neodymium into liquid magnesium between 675 and 800 °C. They observed the formation of a REE-depleted zone at the periphery of the samples, and they correlated the thickness of this zone with the temperature and the treatment duration. Na et al.[23] showed that the extraction efficiency of REEs by liquid magnesium decreased with decreasing the particle size of NdFeB magnet. Neodymium extraction from particle size of 500 µm resulted in the formation of an alloy containing 19% (wt) of neodymium in magnesium after 50 minutes treatment while extraction from particle size of 5 mm resulted in a neodymium content of 24% (wt) under the same experimental conditions. Nam et al.[24] reported the same observation for dysprosium extraction by liquid magnesium from NdFeB

magnets in granular media after 6 to 48 hours of treatment. The particle size influenced the extraction efficiency as 76% (wt) of dysprosium were extracted after 24 hours of treatment when the particle size was lower than 200 µm whereas the extraction efficiency reaches 81% (wt) when the particle size was greater than 2 mm. Likewise, the extraction efficiency reached 97% (wt) of dysprosium after 48 hours when the particles size was greater than 2 mm whereas particle size lower than 200 µm led to 94% (wt) of dysprosium extraction. These authors explained these counterintuitive results by the presence of oxide layers onto the surface of small particles, which negatively affects neodymium and dysprosium extraction.

Sun et al.[25] studied the extraction mechanisms of neodymium from a magnet between 730 and 930 °C at Mg/NdFeB mass ratio ranging from 0.5 to 2.0. The scraps were initially immersed in an aqueous solution of potassium hydroxide (KOH) for 8 hours to remove oil contamination and smudginess. After washing with water and drying at 180 °C, the magnet was mechanically ground with a shredder to produce a powder which the particle size was less than 150 µm. Examination of the extraction rate as a function of the treatment time showed 15 minutes of contact between the magnet and liquid magnesium was enough to reach the steady state for neodymium extraction. Akahori et al.[26] carried out a parametric study of the diffusion of neodymium and dysprosium into liquid magnesium at 1000 °C by considering the same behavior between praseodymium and neodymium. In this study, the magnet powder was obtained by grinding NdFeB magnets so that the particle size ranged between 300 and 700 µm. A complete extraction of neodymium was achieved after 6 hours of treatment when the Mg/NdFeB mass ratio was between 2 and 40. A significant improvement in dysprosium extraction was also observed in the presence of calcium, which reduces rare-earth oxides into rare-earth metals. Park et al.[27] showed that high Mg/NdFeB mass ratio ranging from 6 to 15 improved magnesium penetration into the magnet and, therefore, increased drastically the extraction efficiency of dysprosium from 58% (Mg/NdFeB mass ratio=6) to 66% (Mg/NdFeB mass ratio=15). They pointed out that this ratio is much less critical for neodymium extraction than for dysprosium extraction since neodymium was fully extracted at a Mg/NdFeB mass ratio ratio of 7. Nam et al.[28] performed a detailed study of dysprosium extraction by liquid magnesium. They showed that heat treatment led to the formation of the intermetallic compound Dy_2Fe_{17}, which may diffuse less rapidly into the magnesium. They also showed that dysprosium oxides may diffuse even more slowly, and that elemental diffusion decreases according to the following order: $Dy_2Fe_{14}B$>Dy_2Fe_{17}>dysprosium oxides.

Only a few data of neodymium extraction from magnet into liquid magnesium and growth kinetics of diffusion zone are reported in the literature, and these data concern only experiments performed between 700 and 800 °C in static systems. In the present work, neodymium extraction in liquid magnesium by contacting spent magnet powder prepared by decrepitation with liquid magnesium was investigated between 700 and 900 °C in a perfectly stirred reactor. These operating conditions ensure a homogeneous chemical composition of the liquid phase and prevent the formation of a neodymium concentration gradient near the magnet interface, where a neodymium-enriched liquid boundary layer could slow the extraction rate.

In this work, the growth kinetics of the diffusion zone characterized by neodymium depletion is studied and the time to treat the decrepitated powder using liquid magnesium is estimated to envisage the use of liquid magnesium in industrial process to extract neodymium from spent NdFeB magnets.

2. Materials and methods

Discarded permanent NdFeB magnets from hard disk drives were reduced to powder by hydrogen decrepitation (HD). HD was performed at room temperature under hydrogen (Hydrogen pressure=1 bar). After hydrogenation, the powder was sieved to recover particle which the size was below 200 µm (d_{50}=100 µm). Table 1 gives ICP-MS analyses of the resulting decrepitated powder:

Table 1 Elemental analyses of the NdFeB magnet powder after decrepitation and sieving.

Elements	Fe	Nd	Pr	Dy	B	Others
%(wt)	62.83	23.66	2.90	2.95	1.00	6.66

Sun et al. showed the maximum of neodymium extraction efficiency was reached within 15 minutes when the particle size was less than 149 µm. Therefore, it was expected that neodymium extraction by liquid magnesium may be similar for the decrepitated NdFeB magnet which the particle size was lower than 200 µm. In the present study, it was necessary to slow down the neodymium diffusion to investigate the kinetic growth of the diffusion zone since the steady state was reached too quickly in the experimental setup displayed in Figure 2a. The neodymium diffusion at the magnet/magnesium interface was slow down by sintering the powder produced by decrepitation. Powder was sintered by filling a carbon graphite mold (15 x 20 mm cylinder) in a hot press for 10 hours at 1000 °C and 40 MPa under argon atmosphere (Figure 2b). After sintering, the cylinder was cut into slices of 3 mm thickness to investigate neodymium diffusion at the magnet/magnesium interface (Figure 2c). Each sample was then placed in a stainless-steel capsule measuring 80 x 28 mm (Figure 2d) together with magnesium at a Mg/NdFeB mass ratio of 5. The capsule was carefully sealed by arc welding under argon in a glove box (Jacomex©) which the oxygen content was less than 0.5 ppm.

(a)

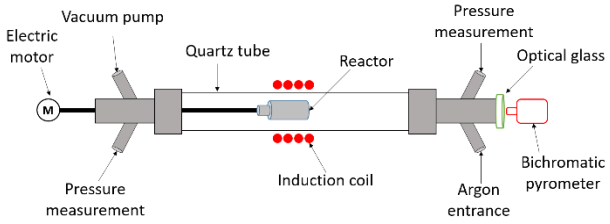

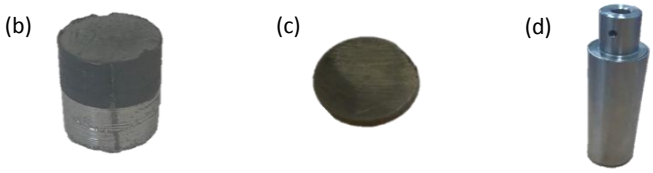

Figure 1 : (a) Experimental setup used for rare-earth elements extraction by liquid magnesium, (b) sintered cylinder of magnet powder, (c) 3 mm-thickness cylindrical sample, (d) Argon sealed capsule containing magnet powder and magnesium.

Bulk densities (ρ_b) of the samples were measured 6 times at 25 °C using a pycnometer (ρ_b =7.71, 7.27, 7.44, 7.78, 7.76, 7.77 g/cm^3). The average value of the bulk density was equal to 7.62 g/cm^3 with a confident interval of 90% at [7.45; 7.80] g/cm^3. According to Sagawa at al., Brown et al. and Xia et al., the true density (ρ_t) of NdFeB magnets is 7.54 g/cm^3 at 25 °C.[29–31] The porosity of the material (ε) can be calculated following the following equation:

$$\varepsilon = 1 - \frac{\rho_b}{\rho_t} \quad (1)$$

The lowest value obtained in the confidence interval was used to estimate the porosity of the material, i.e. ε=1.20%. This value was considered negligible.

The capsule displayed in Figure 2d was held inside an induction coil to heat the sample (Figure 2a). It was attached to a rotating rod driven by an electric motor, which allowed chemical homogenization of the liquid magnesium throughout the treatment and ensured perfectly stirred reactor conditions at 27 rpm. The axis of rotation was inclined at 15° to confine the material at the bottom of the capsule. A quartz tube connected to a vacuum pump (Franklin electric © model 1101006414) and an argon source covered the hot zone to provide inert conditions. A bichromatic pyrometer (Optris©, model OPTCTRF1ML) was used to measure and record the temperature during the experiment. The pyrometer was calibrated by comparing its temperature measurements with the temperatures recorded by two thermocouples located at the side of the capsule and at the vicinity of the location where the pyrometer recorded the temperature. After heating, the magnet was cut into two halves to observe the sample center by scanning electron microscopy after polishing. The samples were polished at 250 rpm on the cut face using silicon carbide grits ranging from 200 µm to 10 µm. Finer polishing was performed using a diamond suspension with particle sizes of 3 µm and 1 µm. Finally, the samples were carefully cleaned in ethanol under ultrasonic agitation for 5 minutes. The concentration profiles in the central zone of the sample where mass transfers occur in a unidirectional manner parallel to the axis of the cylinder were determined by measuring the thickness of the diffusion zone, which is depleted in REEs. These measurements were performed by scanning electron microscopy (Quanta 600). The diffusion zone was identified in each sample by Energy Dispersive Spectrometry (EDS) since the contrast differences observed by EDS is high as shown in Figure 3. This Figure distinguished the (a) diffusion zone, (b) the solidified magnesium (b) and the inner zone of the magnet (c) unaffected by neodymium extraction from the liquid magnesium.

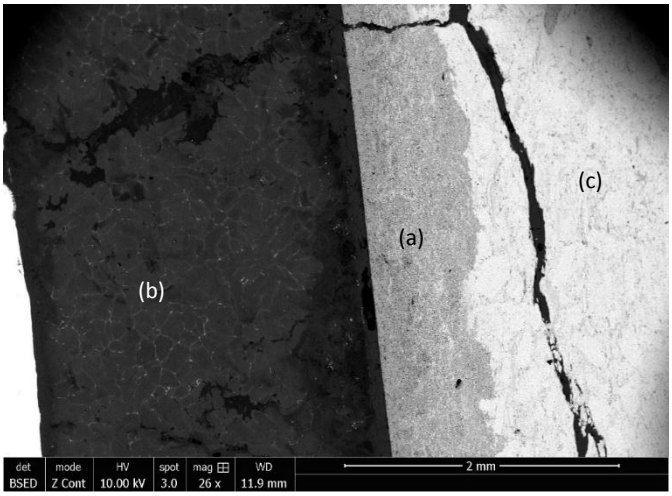

Figure 3: SEM photography of the magnet-magnesium system after extraction at 900 °C for 60 min. (a) diffusion zone, (b) REEs enriched magnesium zone and (c) zone in which the magnet was not affected by diffusion.

SEM pictures have been taken all along the magnet and magnesium interface containing the total diffusion zone thickness of the sample. Diffusion zones on each picture has been truncated using contrast image analysis tool on GIMP software (version 2.10.24) as shown in figure 4. Once the diffusion zone is clearly identified, its thickness can be calculated with the equivalent number of pixels proportionally to the SEM scale used. The average of each estimation for every picture taken for the same sample gives the estimation of the diffusion zone thickness.

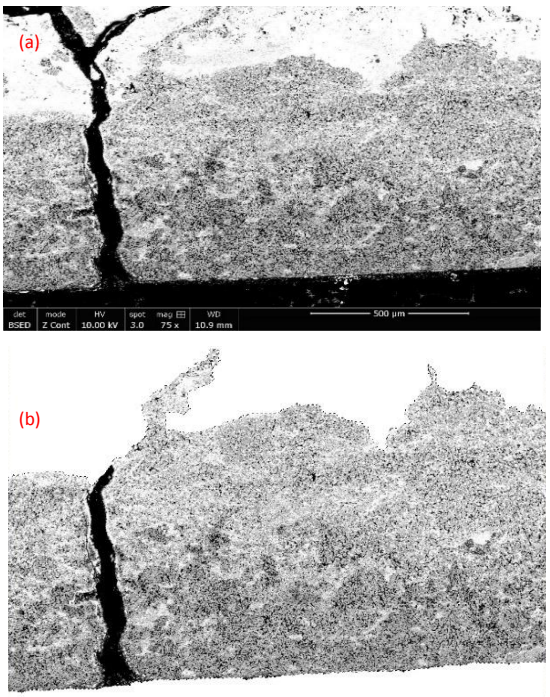

Figure 4: (a) SEM photography of the diffusion zone for image analyses resulting in the identification of (b) the diffusion zone.

3. Results and discussion

3.1 Characterization of the diffusion layer at the magnet-magnesium interface

For this study, nineteen extraction tests were carried out at temperatures ranging from 700 to 900 °C during 15 to 360 minutes. Figure 5 shows the average thickness of the diffusion zone increases with temperature and treatment duration. Therefore, REE transport phenomena in the diffusion layer may be the limiting factor of the extraction mechanism. For the lowest temperature (700 °C), the average thickness of the diffusion zone remains constant until ca. 30-60 min, and then increases. This phenomenon was systematically observed for the three trials at this temperature. Therefore, it was not attributed to the heating ramp or a bias related to temperature measurement. This incubation time was not observed at the other temperatures likely because no data were recorded during the incubation time, which may occur at the very early time.

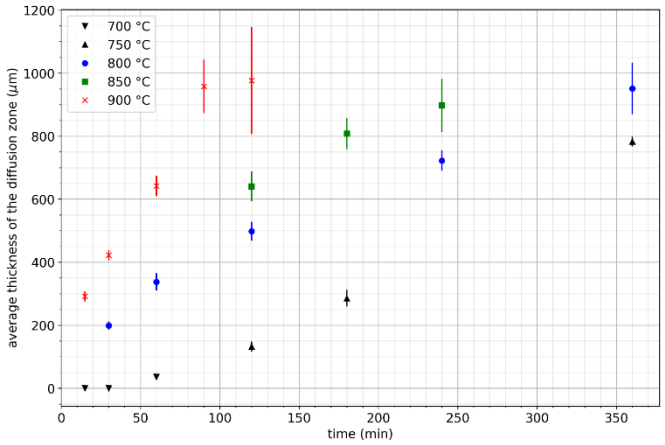

Figure 5: Variation of the average thickness of the diffusion layer during neodymium extraction by liquid magnesium as a function of time between 750 and 900 °C.

SEM pictures showed significant variations in the characteristics of the diffusion layer, as illustrated in Figure 6 after 1 hour of thermal treatment at 800 °C and 2 hours of thermal treatment at 900 °C. Below 750 °C, samples exhibited few diffusion layers scattered at the edge with magnesium and mainly unaffected zones. However, the diffusion layers observed had uniform thickness resulting in a narrow confidence interval of a highly precise average thickness. At higher temperatures, diffusion layers were observed all along the entire sample interface but displaying irregular thickness. This phenomenon became more prominent for thicknesses exceeding 500 µm and led to a decrease of uniformity intensified above 900 µm.

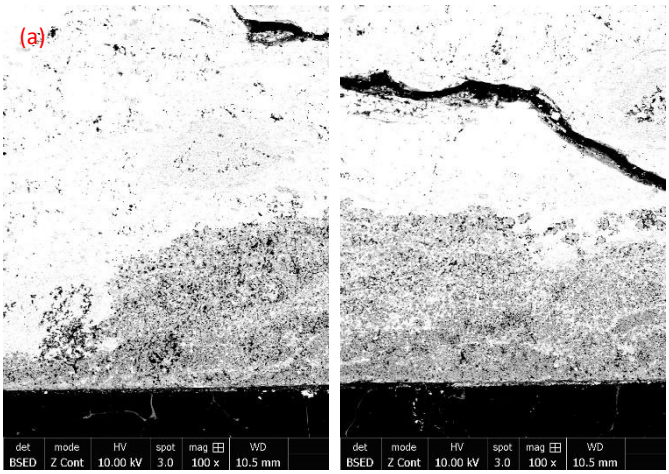

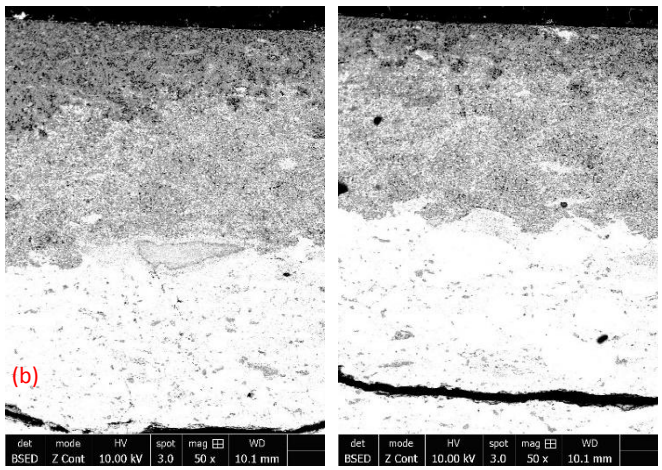

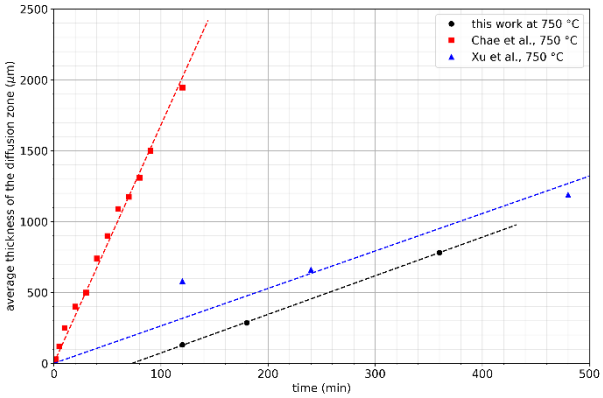

(b)

Figure 6: SEM photography of the diffusion layer obtained at (a) 800 °C for 1 hour (magnitude x 100) and (b) 900 °C for 2 hours (magnitude x 50) with different thicknesses.

Xu et al.[21] and Chae et al.[22] investigated the growth of the diffusion zone during neodymium extraction by liquid magnesium from 700 to 800 °C. Figure 7 compares the experimental data obtained in the present study with those obtained by these authors.

A significant discrepancy is observed between the works of Xu et al. and Chae et al. as the growth rates of the diffusion layer are equal to 1.5 and 12.5 µm.min^{-1} around 700 °C, and 2.6 and 16.8 µm.min^{-1} at 750 °C, respectively. Furthermore, no incubation time was observed by Chae et al. whereas it was not possible to conclude regarding the work of Xu et al. since they did not record data at the earliest time. Above 800 °C, Chae et al. reported a linear increase of the thickness of the diffusion zone up to 2700 µm. Above this value, the thickness increase was not linear, i.e. the growth kinetics of the diffusion layer decreased (Figure 7c).

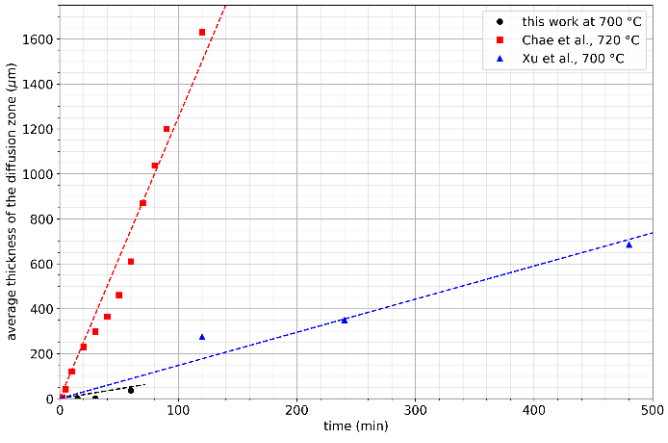

(a)

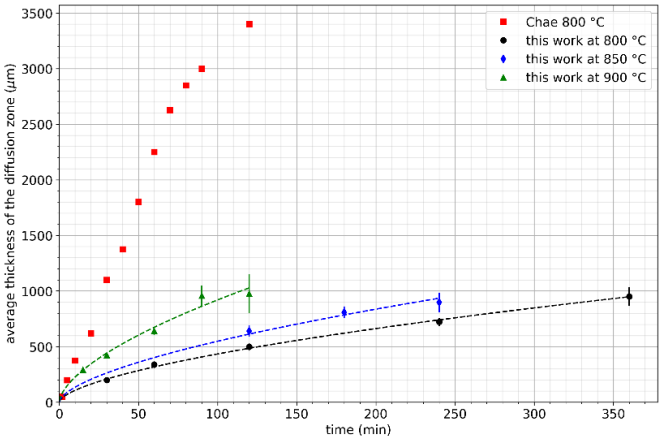

(c)

Figure 7 : Comparison of the diffusion zone growth from the present work with those reported by Chae et al. [22] and Xu et al. [21] at (a) 700-720 °C , (b) 750 °C and (c) at temperatures above 800 °C. The dash lines were calculated by using Eq. (3).

This observation is in fair agreement with the results obtained in the present work even if the values of the thickness of the diffusion zone reported by Chae et al. are higher. The diffusion layer growth remains significantly lower in the present work than that obtained by Chae at 800 °C and even at 900 °C. This significant discrepancy between the present results and those reported in the literature may be explained by differences in the preparation of the sintered magnets used in this work. SEM observations revealed the presence of magnesium in the diffusion layer as it was found by Xu et al. and Chae et al. This can be due to diffusion, but also because of magnesium infiltration, the latter being particularly influenced by the magnet porosity. As mentioned above, the magnet powder was sintered under severe conditions to achieve negligible porosity in the massive sample. As a consequence, mechanisms of magnesium infiltration are drastically limited, allowing to observe on a large scale the extraction kinetics that would be obtained at the powder scale. Finally, this approach allows to extrapolate results to the decrepitated powder particle size scale. The following empirical law can be used to describe the evolution of the thickness of the diffusion zone as

a function of time and temperature at temperatures greater than 800 °C as shown in figure 7:

$$l(t,T) = A(T)t^{0.61} \quad (2)$$

Where A(T) is an empirical parameter (A(800 °C)= 26.2 µm.min$^{-0.61}$, A(850 °C)= 33.0 µm.min$^{-0.61}$ and A(900 °C)= 55.4 µm.min$^{-0.61}$. The explanation of the underlying mass transfer phenomena will require further investigations to provide a more detailed modelling of the kinetic of the diffusion layer growth. However, this initial approach is sufficient to perform preliminary calculations regarding the treatment duration required for REEs extraction in decrepitated magnet powder for industrial perspective.

3.2 Estimation of the duration of the neodymium extraction by liquid magnesium

The duration of the treatment to fully extract neodymium with liquid magnesium from the powder produced by magnet decrepitation can be estimated by considering the growth of the diffusion layer at the interface between the magnet and liquid magnesium. For this aim, the particle size distribution of the decrepitated powder was modelled by using the Rosin-Rammler equation[32] and by assuming a sieve size of 500 µm:

$$Y = \min\left(1, \frac{1 - exp\left(-\left({}^{D}/_{D_n}\right)^{n}\right)}{1 - exp\left(-\left({}^{D_{max}}/_{D_n}\right)^{n}\right)}\right) \quad (3)$$

where Y represents the fraction of size smaller than the diameter D, D_n is the characteristic diameter of the particle population, D_{max} is the maximum diameter of the particles, and n denotes for the dispersion of the particle size distribution. According to Rivoirard et al.[6], the particle size distribution can reasonably be described by the Rosin-Rammler equation by considering D_n = 3.5 10^{-4} m, D_{max} = 5 10^{-4} m and n = 2.5. Figure 8a shows the volume fraction passing and figure 8b the density of the volume fraction as a function of particle size distribution calculated by using Eq. (3).

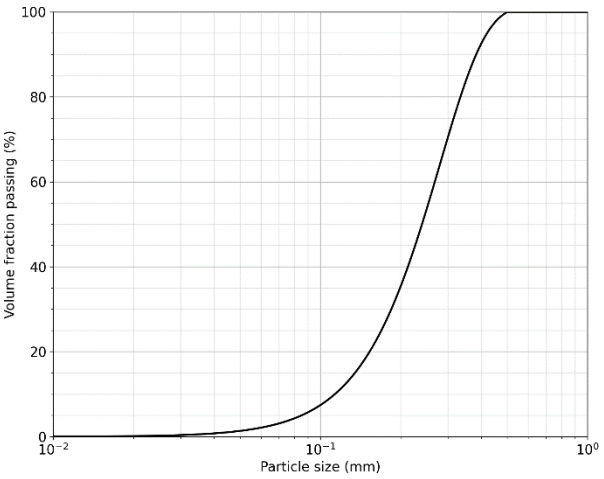

(a)

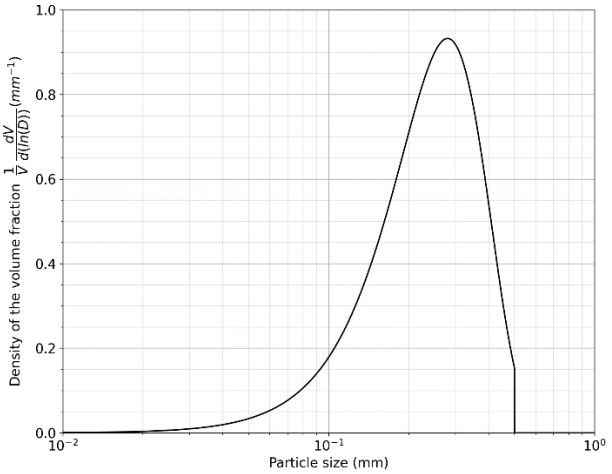

(b)

Figure 8: (a) Volume fraction passing and (b) density of the volume fraction as a function of particle size distribution of powder produced from decrepitated magnet calculated by the Rosin-Rammler equation.

By using the estimated growth rate of the diffusion layer, the volume fraction of treated powder can be expressed as a function of temperature and time. For this purpose, it was assumed that each grain was a sphere of diameter D and that neodymium extraction by liquid magnesium was responsible for the formation of a diffusion zone l(T,t) in the treated volume fraction ($x_{treated}$) of such a grain defined by:

$$\text{If D < 2 l(T,t) then } x_{treated} = 1 \quad (4)$$

$$\text{If D >2 l(T,t) then } x_{treated} = \left(1 - \left(\frac{D - 2l(T,t)}{D}\right)^3\right) \quad (5)$$

From Eqs (4) and (5), it is thus possible to calculate the remaining volume fraction of the untreated powder ($x_{untreated}$):

$$x_{untreated}(\mathrm{T,t}) = \int_0^{D_{max}} \left(1 - \left(\frac{D - 2l(T,t)}{D}\right)^3\right) \frac{dY(D)}{dD} dD$$

Figure 9 shows the volume of residual untreated powder as a function of temperature and extraction time. The treatment can be relatively short to extract neodymium by liquid magnesium since less than 22 minutes is enough whatever the temperature as it was reported by Na et al.[23]. Temperature represents a critical parameter on the treatment duration. A decrease of 100 °C, from 900 °C to 800 °C, results in an increase of the treatment duration of 250%, from 6 to 22 minutes, to reach 99.9% of treated powder.

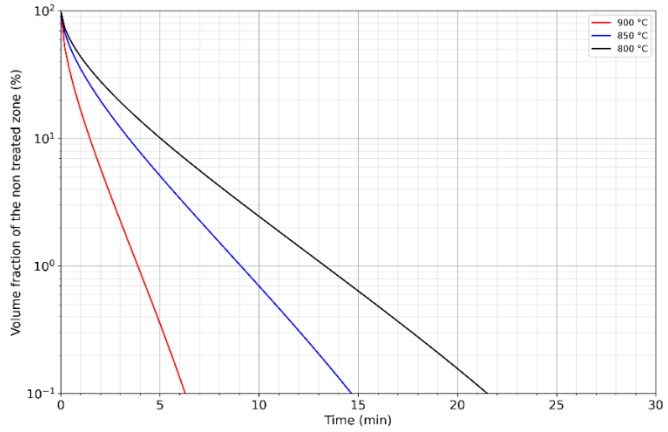

Figure 9 : Modelling of the volume fraction of residual untreated powder as a function of temperature and immersion time in liquid magnesium.

In addition, the target fraction to be treated influences strongly the treatment duration. For example, the treated volume fraction can reach 90% of the material if the treatment duration lasts between 1.5 and 5 minutes depending on the temperature, while a target of 99% would multiply the treatment duration by 2.5.

These preliminary calculations show that this extraction method could be considered for industrial use to extract REEs from decrepitated powders. Complementary studies could also be carried out at higher temperatures. Nevertheless, performances obtained at 900 °C are presently highly attractive and could stand for an optimum range of temperature for such a process treatment.

4. Conclusions

In this paper, a laboratory-scale equipment specifically designed for liquid magnesium extraction (LME) of REEs from used NdFeB magnets decrepitated under hydrogen has been presented. The set of experiments conducted between 700 and 900 °C during 30 minutes to 6 hours allowed characterizing the growth kinetics of the REE-depleted zone at the magnetmagnesium interface. The treatments have been carried out on massive samples sintered from a decrepitated powder under severe operating conditions to eliminate internal porosities. The lack of porosity avoids infiltration of liquid magnesium. Under these conditions, the kinetic laws at macroscopic scale can be used to simulate the neodymium extraction by liquid magnesium on decrepitated powder. High consistency with the work of Xu et al. was obtained while high discrepancies were observed with the data reported by Chae et al. Such discrepancies may be explained by the difference of porosity between the materials used in the present work and the material used in the work of Chae et al. The results provide important insights for the determination of the treated volume fraction and give preliminary indications of the industrial performance of REEs extraction from spent magnets by liquid magnesium. This work used an empirical model describing the froth kinetic of the diffusion layer of neodymium combined with the Rosin-Rammler equation to estimate the optimal the duration of liquid magnesium extraction to extract efficient extraction of neodymium from decrepitated magnet by liquid magnesium. In conclusion, there is a need for additional research to enhance the understanding of the extraction mechanisms. For instance, conducting a comprehensive characterization using an electron probe micro-analyser would enable more accurate concentration measurements of REEs and magnesium in the diffusion layer. This, in turn, would provide a more detailed description of the mass transfer phenomena occurring in this zone.

Author Contributions

Conceptualization: TQ, AC; Formal analysis: TQ, AC, NS, JM; Funding acquisition: AC; Investigation: NS, JJ; Project administration: AC, TQ; Supervision: TQ, AC; Visualization: NC; Writing-original draft: NC, TQ; writing-review and editing: AC, TQ.

Conflicts of interest

The author declares no conflict of interest.

Acknowledgements

The author would like to acknowledge the Lorraine University of Excellence, the LabEx RESSOURCES21 and the LabEx DAMAS for their financial supports. The author expresses his gratitude to Sophie Rivoirard from MagREEsources start-up for furnishing the decrepitated magnet powder and for her support and the enriching discussions as well as Emma Khebchi student from University of Mans for the work done for the experimental section.

Notes and references

1 H. Jin, P. Afiuny, S. Dove, G. Furlan, M. Zakotnik, Y. Yih and J. W. Sutherland, *Environ. Sci. Technol.*, 2018, **52**, 3796–3802.
2 R. Skomski, in *Novel Functional Magnetic Materials*, ed. A. Zhukov, Springer International Publishing, Cham, 2016, vol. 231, pp. 359–395.
3 Alves Dias, *The role of rare earth elements in wind energy and electric mobility: an analysis of future supply/demand balances.*, Publications Office, LU, 2020.
4 Gielen Dolf and Lyons Martina, .
5 J. H. Rademaker, R. Kleijn and Y. Yang, *Environ. Sci. Technol.*, 2013, **47**, 10129–10136.
6 S. Rivoirard, J. G. Noudem, P. de Rango, D. Fruchart and S. Liesert, .
7 P. Dalmas de Réotier, D. Fruchart, P. Wolfers, P. Vulliet, A. Yaouanc, R. Fruchart and P. L'Héritier, *J. Phys. Colloques*, 1985, **46**, C6-249-C6-251.
8 D. Book and I. R. Harris, *Journal of Alloys and Compounds*.
9 J. M. Cadogan and J. M. D. Coey, *Applied Physics Letters*, 1986, **48**, 442–444.
10 V. A. Yartys, A. J. Williams, K. G. Knoch, P. J. McGuiness and I. R. Harris, *Journal of Alloys and Compounds*, 1996, **239**, 50–54.

11 M. Zakotnik, E. Devlin, I. R. Harris and A. J. Williams, *Journal of Iron and Steel Research, International*, 2006, **13**, 289–295.
12 R. Nakayama and T. Takeshita, *Journal of Alloys and Compounds*, 1993, **193**, 259–261.
13 H. Sepehri-Amin, W. F. Li, T. Ohkubo, T. Nishiuchi, S. Hirosawa and K. Hono, *Acta Materialia*, 2010, **58**, 1309–1316.
14 S. Sugimoto, *J. Phys. D: Appl. Phys.*, 2011, **44**, 064001.
15 M. Nakamura, M. Matsuura, N. Tezuka, S. Sugimoto, Y. Une, H. Kubo and M. Sagawa, *Appl. Phys. Lett.*, 2013, **103**, 022404.
16 R. S. Sheridan, A. J. Williams, I. R. Harris and A. Walton, *Journal of Magnetism and Magnetic Materials*, 2014, **350**, 114–118.
17 T. Horikawa, M. Yamazaki, M. Matsuura and S. Sugimoto , *Science and Technology of Advanced Materials*, 2021, **22**, 729–747.
18 I. Poenaru, E. A. Patroi, D. Patroi, A. Iorga and E. Manta, *Journal of Magnetism and Magnetic Materials*, 2023, **577**, 170777.
19 M. K. Jha, A. Kumari, R. Panda, J. R. Kumar, K. Yoo and J. Y. Lee, .
20 M. Z. Rasheed, S.-W. Nam, J.-Y. Cho, K.-T. Park, B.-S. Kim and T.-S. Kim, *Metall Mater Trans B*, 2021, **52**, 1213–1227.
21 Y. Xu, L. S. Chumbley and F. C. Laabs, *J. Mater. Res.*, 2000, **15**, 2296–2304.
22 H. J. Chae, Y. D. Kim, B. S. Kim, J. G. Kim and T.-S. Kim, *Journal of Alloys and Compounds*, 2014, **586**, S143–S149.
23 H. W. Na, Y. H. Kim, H. Taek Son, I. Ho Jung, H. Shin Choi and T. Bum Kim, *CNANO*, 2014, **10**, 128–130.
24 S.-W. Nam, M. Z. Rasheed, S.-M. Park, S.-H. Lee, D.-H. Kim and T.-S. Kim, 4.
25 M. Sun, X. Hu, L. Peng, P. Fu, W. Ding and Y. Peng, *Journal of Materials Processing Technology*, 2015, **218**, 57–61.
26 T. Akahori, Y. Miyamoto, T. Saeki, M. Okamoto and T. H. Okabe, *Journal of Alloys and Compounds*, 2017, **703**, 337–343.
27 S. Park, S.-W. Nam, J.-Y. Cho, S.-H. Lee, S.-K. Hyun and T.-S. Kim, 5.
28 S.-W. Nam, S.-M. Park, M. Z. Rasheed, M.-S. Song, D.-H. Kim and T.-S. Kim, *Metals*, 2021, **11**, 1345.
29 M. Sagawa, S. Fujimura, H. Yamamoto, Y. Matsuura and K. Hiraga, *IEEE Trans. Magn.*, 1984, **20**, 1584–1589.
30 D. Brown, B.-M. Ma and Z. Chen, *Journal of Magnetism and Magnetic Materials*.
31 M. Xia, A. B. Abrahamsen, C. R. H. Bahl, B. Veluri, A. I. Søegaard and P. Bøjsøe, *Journal of Magnetism and Magnetic Materials*, 2017, **441**, 55–61.
32 M. Alderliesten, *Particle Particle Systems Characterization*, 2013, **30**, 244–257.